

# How a new electromagnetic surface treatment can reduce resistance to motion of a displacement yacht

---

## Authors

Melegari A.<sup>(1)</sup>, Aspesi D.<sup>(2)</sup>, Tincani E.<sup>(3)</sup> and Poggianella M.<sup>(4)</sup>.

<sup>(1)</sup> Degree in Physics, Responsible for Physics Research, SOP srl, Busto Arsizio (VA), Italy

<sup>(2)</sup> Engineer, Industry Brand Manager, SOP srl, Busto Arsizio (VA), Italy

<sup>(3)</sup> Naval Architect and Marine Engineer, Genoa, Italy

<sup>(4)</sup> SOP Technology Developer, SOP srl, Busto Arsizio (VA), Italy

## Abstract

Mechanical friction can be interpreted on an atomic level as the result of the contribution of adhesion and cohesion forces. Ultimately, these forces are generated by electromagnetic interaction at the contact surface of two bodies.

The work described in this paper is based on this approach, studying the influence of a new treatment on a model of a displacement yacht reproduced on a 1:20 scale, painted with standard naval paint. The model underwent a series of towing tests by University of Genoa to determine its resistance to motion, at a velocity of approximately 9, 12, 15, 18, 21 and 24 kn (in Froude similitude). The entire yacht model was subsequently treated with an innovative physics based process developed by the company SOP srl. The treatment consists of the transferral of electromagnetic waves, at specific frequencies, to the target. The process, by means of this electromagnetic field, modifies the molecular forces of adhesion, responsible for the friction between the target material and the water. The aim of the treatment applied to the model was to obtain a reduction in its friction with water. The tests were, therefore, repeated on the same displacement yacht after treatment.

A yacht's total resistance to motion ( $C_t$ ) can be considered as the result of resistance due to friction ( $C_f$ ) and the so called residual resistance

( $C_r$ ). The latter component depends mostly on the shape of the craft. The analysis of the results was made under the assumption that the only component undergoing changes due to the process is  $C_f$ . The treatment, in fact, does not modify the shape of the craft or the roughness of the surface. The results highlight an average improvement of the friction coefficient of between 1 and 5% (as the mean value of 2 trials for each "run"), depending on the Froude Number. The greatest gain was obtained for Froude numbers of between 0.4 and 0.6. In fact, the  $C_r$  contribution is greater at lower speeds. Whilst, at other velocities there is a reduction in the relevance of the resistance contribution due to friction. Results seem to suggest that the special treatment applied can produce an improvement in the total hydrodynamic behaviour, in the form of a significant reduction in the resistance to motion due to friction.

The satisfactory outcome of this study has stimulated further in depth tests on flat plates, which will be conducted in the future, to investigate the efficacy of the treatment for higher Reynolds numbers.

## Keywords

Friction, surface treatment, physical process, hydrodynamic, resistance to motion, adhesion.

## Introduction

Friction is one of the most studied phenomena in fluid dynamics, because of its effects on laminar or turbulent motion.

The classic approach (1-3) is generally utilised. It is based on Newton's laws, and it considers friction as a particular force (proportional to speed rather than to its derivative), which tends to oppose the motion of an object immersed in a fluid, reducing its speed.

The purpose of this study is to suggest an approach that aims at no longer seeing the fluid dynamics friction as a macroscopic phenomenon, related to a force affecting the speed of an object, but as the resultant of inter-atomic interactions.

All the physics research over the last century, in fact, has re-interpreted mechanics, including the concept of force as the resultant of interactions that occur on a microscopic scale. These interactions can be divided into four main classes: electro-magnetic, strong nuclear, weak nuclear and gravitational interactions.

They are the result of interference between the characteristic waves of the considered systems. In fact, according to de Broglie's equation, every particle oscillates with a specific wavelength, given as:

$$\lambda = \frac{h}{mv}$$

(where  $h$  is Planck's constant,  $m$  mass and  $v$  velocity).

In the case of complex systems, made up of several particles, the composition of the characteristic waves defines the field associated with the system itself.

Based on the interference principle (whose analogue in classical mechanics is the action-reaction principle), the fields that are generated by two materials on an atomic level interfere with each other, giving origin to the commonly known macroscopic forces: from Van der Waals forces, to London dispersion forces, to binding or aggregation forces (4, 5). Ultimately, the fields are responsible for the chemical and physical characteristics of the systems analysed and for the interactions between them.

In this specific case, friction is considered as the resultant of the interaction between two surfaces (the one of the model yacht and the one of the fluid in which the hull is immersed), and among the atoms closer to this interface (i.e. boundary layer (6)). These interactions are

commonly observed and catalogued as adhesion and cohesion forces (7-9).

In the study of friction reduction in a fluid, the works based on the classical mechanical approach focus their attention on making the surface as smooth as possible to the friction forces, or else, on modifying the shape of the ship. The goal of the trials performed in this work, instead, is not to make the hull exempt from the action of external forces, but to act directly on the interactions that originate at the point of, and in the proximity of, the solid-liquid interface between the atoms of the hull's surface and those of the water where the hull is immersed and moves.

The Sirio Operating Process<sup>®</sup> technology, used to treat the model hull, object of the series of tests described in this paper, operates directly on the field naturally generated by the particles which make up the material. It provides the target with an informative contribution, by creating strongly coherent electro-magnetic fields that can modulate, through an interference mechanism, the response of the system to which they are applied, to obtain the desired result: in this case the decrease in the friction with water.

Considering motion in a fluid medium, both laminar or turbulent, the friction in the water is mainly caused by the molecules closer to the interface between the immersed body and the fluid. For example, the friction in a laminar motion of an immersed body can be expressed as

$$\frac{F}{Area} = -\mu \frac{\Delta V}{\Delta y}$$

*Equation 1: Newton's formula for friction in a fluid*

whose parameters are described in figure 1, and  $\mu$  is the viscosity of the fluid.

According to this interpretation scheme, the friction phenomenon originates at the interface between the immersed body and the fluid, to spread subsequently to the more distant water layers.

The SOP technology treatment is based on the same idea of this chain of interactions. The information spreads from the model to the water molecules in contact with it, and then on to the more distant layers.

The reduction of the inter-atomic interactions at the interface between the hull and the water, and of those among the contiguous water molecules leads to a reduced binding resistance, and consequently to a better flow within the liquid.

## Materials and Methods

The model of a displacement yacht was manufactured on a 1:20 scale, by the machining of a polyurethane resin block. The principal characteristics of the model are summarised in the following table (table 1). The values of the life-size equivalent boat are also included.

	Model dimensions	Life-size dimensions
<b>Δ (mass)</b>	13,415kg	110T
<b>Length at waterplane</b>	1,247m	24,941m
<b>Draft (front)</b>	0,073m	1,464m
<b>Draft (back)</b>	0,073m	1,464m
<b>θ long (trim angle)</b>	0°	0°
<b>Wetted surface</b>	0,517m <sup>2</sup>	206m <sup>2</sup>

Table 1: Dimensions of model and equivalent life size boat

The model was painted and finished with a standard covering applied by an important paint manufacturing company.

The model was, then, prepared in the Towing Tank Laboratory of DINAV (Department of Naval Industry) at the Università degli Studi di Genova. (Genoa, Italy) and trimmed by means of two laser meters.

The tank's main characteristics are: 60m approx length, 2.8m width, 1.8m average depth. The velocity was recorded by a tachometer wheel with an encoder and notches on the rails. The resistance to motion was measured using a load cell with an end of scale reading of 10kg. All the results and data were recorded on an industrial PC with a DAQ National Instrument board.

According to the test protocol, the model underwent two series of runs to determine its resistance to motion before and after treatment. The series of tests were made up of 6 runs, each with a different Froude number (Fn), at the following values: 0.3 Fn – 0.4 Fn – 0.5 Fn – 0.6 Fn – 0.7 Fn – 0.8 Fn.

According to equation 2

$$F_n = \frac{V}{\sqrt{g \cdot L}}$$

$$\text{where } \begin{cases} V = \text{Velocity [ m/s]} \\ g = \text{Acceleration of gravity [ m/s}^2\text{]} \\ L = \text{Length [ m]} \end{cases}$$

Equation 2: Definition of Froude number

Equation 2: Definition of Froude number

the model was therefore towed at a velocity of (in Froude similitude) approximately 9, 12, 15, 18, 21 and 24kn.

The model was then carried to the SOP premises to be treated with the innovative SOP Technology. This technology has been successfully applied to different fields, such as inorganic matter, plants and animals (10-12).

The treatment is based on a principle of quantum physics that states that every system is characterised by specific wavelengths. These wavelengths correspond to specific information, and consequently to specific functions. The technology consists in identifying the wavelength corresponding to the desired function, and in studying another that is able to interfere with the original, enhancing or inhibiting its intensity. The final step is to transfer this wavelength to a chosen material (carrier) that would then be able to generate a field spreading out its effects to the surrounding environment. The carrier can be chosen from a large variety of materials, thus allowing the technology to be tailored to the specific application.

For this work, the wavelengths responsible for the molecular forces of adhesion and cohesion in water were identified. The treatment was calibrated to associate to the target material (the model yacht) an electromagnetic field that could interfere with the characteristic wavelengths of the water, reducing the forces generated, responsible for friction.

The model was then processed with this technology, and underwent a second series of tests, with the same course as the untreated model. The results were recorded and a correction was made to take into account the different temperatures at which the trials were performed.

The data referring to each series of runs are reported in the following table (table 2), where Nk stands for untreated (Naked) model, Pt for treated (Painted) model and 0 and 1 refer to the two different trials.

	Series Nk_0	Series Nk_1	Series Pt_0	Series Pt_1
T (°C)	16	19	22	22
Dist Laser (mm)	960	960	910	910
Diff L Prow (mm)	272	272	280	280
Diff L Stern (mm)	15	15	65	65
Visc (10 <sup>-6</sup> m <sup>2</sup> /s)	1.1099	1.1099	0.9574	0.9574
Density (kg/m <sup>3</sup> )	998.9	998.9	997.7	997.7
g (m/s <sup>2</sup> )	9.81	9.81	9.81	9.81

Table 2: Data of the different series

It is possible to determine a value of resistance to motion of the model being tested in the tank and then, through the use of similarity models, calculate the real value of resistance. This procedure, defined by ITTC (13), allows the identification and separation of the resistance due to friction of the wetted surface and to the shape of the model, from the resistance owing to the generation of waves.

The evaluation and separation of these types of resistance to motion is generally defined using adimensional coefficients of resistance and can be summarised as  $C_t = C_f + C_r$  where the subscript identifies the type of resistance being considered, t total resistance, f friction resistance, r residual resistance.

$C_t$  is measured by means of the load cell in all the series of runs.  $C_f$  for the untreated model is calculated according to the ITTC procedure, using the resistance curve of the equivalent flat plate, there defined as:

$$C_{fNk}(T) = 0.075 / (\log_{10}(Rn) - 2)^2$$

Equation 3: theoretical value of  $C_f$

where  $Rn$  is the Reynolds number. This allows the determination of the value of  $C_r$  for the untreated model yacht. It is possible, however, to assume that the value of  $C_r$  remains constant for both series on the treated and untreated models, considering that the electromagnetic treatment studied does not entail modifications to the surface or to the shape of the model. We can then calculate the value of  $C_f$  for the treated model, which is the component of the total resistance to motion that will be affected by the proposed process.

Later on, the value  $\Delta C_f\%$  will be utilised which is calculated as the ratio:

$$C_{fPt}(T_{Pt}) / C_{fNk}(T_{Pt}),$$

Equation 4: Expression of percentage variation of  $C_f$

where the subscript  $Pt$  identifies the model after treatment,  $Nk$  the model before treatment, and  $T_{Pt}$  is the temperature during the tests on the treated model. More precisely, this is the comparison between the friction coefficient of the treated model during the tank test and the value calculated at the same temperature according to the ITTC'57 procedure.

## Results and discussion

The results of the total resistance to motion of all the series of runs are shown in tables from 3 to 6, in the appendix.

The graphs summarise the data.

In graph 1 it is possible to see that the trends in the model's behaviour were very regular in all the tests, in the entire range of velocities. It is already possible to see how the trials with the model after treatment show a lower total resistance to motion. Differences in the overall behaviour are evident, and reach their maximum at a velocity of between 0.5 and 0.6  $F_n$ .

In order to better evaluate the influence of the treatment, the contribution of the resistance to motion due to friction, i.e.  $C_f$ , was investigated.  $C_f$  in the treated model was calculated as a difference between  $C_t$ , derived from the measurements, and  $C_r$ . This latter component was calculated from the measurements of  $C_t$  in the runs of the untreated model and the theoretical values of  $C_f$ , as explained above.

Graph 2 shows the variation of  $C_f$  in function of the Froude Number, for the four series of runs. The curves representing  $C_f$  for the untreated model derive from the theoretical model, according to the ITTC '57 procedure. It is important to notice how the experimental curves obtained for the resistance to motion due to friction show a similar behaviour, with a trend that approaches that of the theoretical model. Two interpolating curves were calculated for the series of the treated model, discarding the values that were considered inhomogeneous from the others (i.e. the first point in the first series, and the third point in the second series). From those, a mean curve was calculated, which is shown in the graph (blue line with triangle markers).

It can be noticed that the average results are always below the reference.

Graph 3 shows the percentage variation of  $C_f$  in the treated model with respect to the untreated model (as defined in equation 4), there considered as reference. The results highlight how the treated model shows a significant reduction in resistance to motion due to friction in the entire range of velocities. The highest results were obtained for Froude Numbers of 0.5 and 0.6, corresponding to velocities of 15 and 18kn (in Froude similitude).

## Conclusions

The good results obtained in this study comply with the theory that it is possible to modify the macroscopic effect of microscopic interactions, by means of specific electromagnetic fields, which are associated to the chosen materials that act as carriers, interfering with the ones naturally present. In this work, the associated fields were responsible for the modification of the adhesion and cohesion interactions between the model yacht (used as carrier) and water, at the basis of the friction force. The result was a substantial decrease in the coefficient of resistance due to friction, of 3% on average, with peaks of about 5%. The best results were obtained in a velocity range (of between 12 to 18 kn, in Froude similitude) which is typical for example of private yachts.

At lower speeds, the results were more strongly influenced by possible errors. While at higher velocities there is a reduction in the relevance of the resistance contribution due to friction.

Considering that the component due to friction corresponds in general to half of the total resistance to motion, the proposed treatment can signify an overall reduction of 2% in driving force. This will correspond to significant reductions in fuel consumption and pollutant emissions, a pressing issue nowadays.

In fields where performance is a key to success, such as competition boats (e.g. canoes, sailing boats, etc.), where the form factor is already optimised, important reduction in friction can lead to a remarkable increase in motion velocity.

This treatment, moreover, does not entail any modification of the surface at the interface between the body and the water. Nor does it require the use of special materials. This allows the treatment to be employed to virtually any application where friction with a fluid medium is involved.

Further investigations will be carried out to verify its applicability to other fields and to study improvements in the treatment itself.

One of the next works will be on flat plates, in order to investigate the effects of the SOP treatment on the friction in a system where resistance due to form factor is negligible. This will allow investigations to be carried out at higher Reynolds numbers, thus extending the results to motion at greater speeds.

Moreover, in the course of the new experiments, refining and improvement of the treatment will be performed. The aim of this process is to fine-tune the SOP treatment for different systems operating in different conditions.

## References

1. H. Lamb, *Hydrodynamics*, Cambridge University Press, 1987
2. D. Spataro, *Trattato teorico e pratico di idromeccanica*, U. Hoepli, 1915
3. L.D. Landau, E.M. Lifshitz, *Fluid mechanics*, Pergamon Press, 1959
4. J. Kotz, P. Treichel jr, R.F. Weaver, *Chimica*, Edises, 2007
5. A.J. Stone, *The theory of intermolecular forces*, Paperback, 1997
6. L. Prandtl, *Über Flüssigkeitsbewegung bei sehr kleiner Reibung*, 1904
7. L.D. Landau, *Fisica Statistica*, Editori Riuniti, 1978
8. A.J. Kinloch, *Adhesion and adhesive science and technology*, Chapman and Hall, 1987
9. J. Comyn, *Adhesion science*, Royal Society of Chemistry Paperback, 1997
10. A. Arpinelli et al, *Evaluation of control measures for Clostridial diseases in dairy cattle*, Acts of the Italian Buiatrics Society, Teramo National Congress, 2005, Collection of scientific papers, www.sopgroup.com
11. A. Zanierato, P. Buzzini, *Efficacy of a Bio-Hygienization Additive in Controlling the yeast-like microalga Prototheca zopfii*, NMC 46<sup>th</sup> Annual Meeting, 2008, Collection of scientific papers, www.sopgroup.com
12. A. Centinaio et al, *Case study: improvement of recovery and hydration status in endurance horses by oral administration of a new feed additive: SOP EQWHITE*, ESVCN Congress, 2009, Collection of scientific papers, www.sopgroup.com
13. ITTC, *Recommended Procedures and Guidelines*

## Appendix

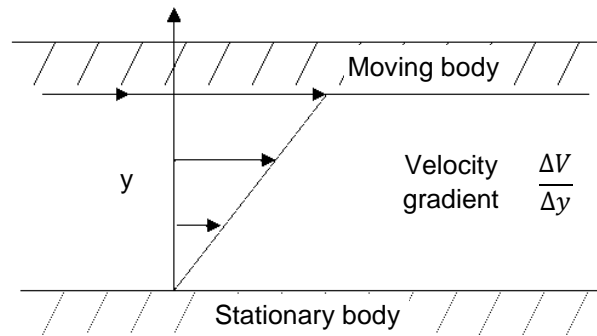


Figure 1: Newtonian approach to friction in a fluid medium

<b>Fn (requested)</b>	<b>v [m/s]</b>	<b>Fn (real)</b>	<b>Rt [N]</b>	<b>C<sub>t</sub></b>	<b>Rn (10<sup>-6</sup>)</b>	<b>C<sub>f NK_0</sub></b>	<b>C<sub>r</sub></b>
0.3	1.06	0.302	1.751	6.06E-03	1.19	4.52E-03	1.54E-03
0.4	1.41	0.403	4.423	8.62E-03	1.58	4.25E-03	4.36E-03
0.5	1.76	0.503	10.961	1.37E-02	1.98	4.06E-03	9.64E-03
0.6	2.11	0.603	14.653	1.27E-02	2.37	3.92E-03	8.83E-03
0.7	2.46	0.703	15.882	1.02E-02	2.76	3.80E-03	6.36E-03
0.8	2.83	0.808	16.848	8.18E-03	3.17	3.70E-03	4.47E-03

Table 3: Results of the first series of tests, untreated model

<b>Fn (requested)</b>	<b>v [m/s]</b>	<b>Fn (real)</b>	<b>Rt [N]</b>	<b>C<sub>t</sub></b>	<b>Rn (10<sup>-6</sup>)</b>	<b>C<sub>f NK_1</sub></b>	<b>C<sub>r</sub></b>
0.3	1.06	0.303	1.818	6.27E-03	1.29	4.44E-03	1.83E-03
0.4	1.41	0.403	4.407	8.59E-03	1.71	4.19E-03	4.40E-03
0.5	1.75	0.500	10.971	1.39E-02	2.12	4.01E-03	9.87E-03
0.6	2.11	0.603	14.682	1.28E-02	2.56	3.86E-03	8.92E-03
0.7	2.46	0.703	15.820	1.01E-02	2.98	3.75E-03	6.38E-03
0.8	2.81	0.803	16.734	8.21E-03	3.41	3.65E-03	4.56E-03

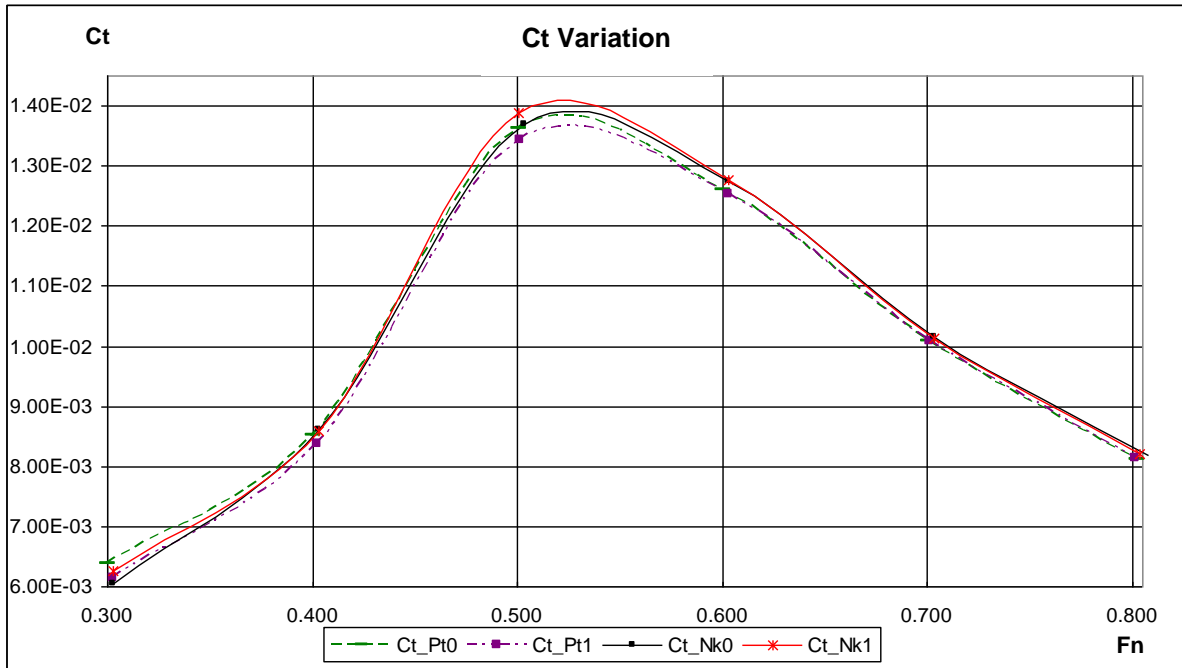
Table 4: Results of the second series of tests, untreated model

<b>Fn (requested)</b>	<b>v [m/s]</b>	<b>Fn (real)</b>	<b>Rt [N]</b>	<b>C<sub>t</sub></b>	<b>Rn (10<sup>-6</sup>)</b>	<b>C<sub>f Pt_0</sub></b>	<b>C<sub>r</sub></b>
0.3	1.05	0.300	1.813	6.38E-03	1.37	4.70E-03	1.67E-03
0.4	1.40	0.400	4.310	8.53E-03	1.82	4.04E-03	4.49E-03
0.5	1.75	0.500	10.767	1.36E-02	2.28	3.88E-03	9.75E-03
0.6	2.10	0.600	14.325	1.26E-02	2.73	3.66E-03	8.94E-03
0.7	2.45	0.700	15.606	1.01E-02	3.19	3.61E-03	6.47E-03
0.8	2.81	0.802	16.477	8.12E-03	3.65	3.55E-03	4.57E-03

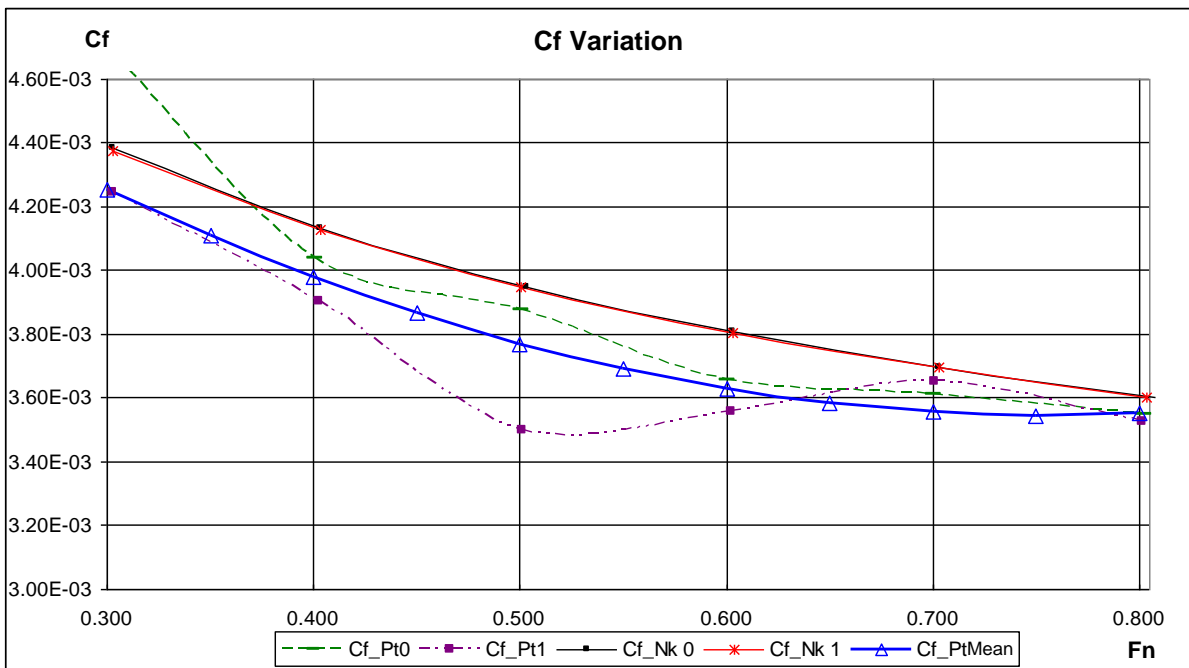
Table 5: Results of the first series of tests, treated model

<b>Fn (requested)</b>	<b>v [m/s]</b>	<b>Fn (real)</b>	<b>Rt [N]</b>	<b>C<sub>t</sub></b>	<b>Rn (10<sup>-6</sup>)</b>	<b>C<sub>f Pt_1</sub></b>	<b>C<sub>r</sub></b>
0.3	1.06	0.303	1.779	6.14E-03	1.38	4.25E-03	1.89E-03
0.4	1.41	0.402	4.275	8.37E-03	1.83	3.90E-03	4.46E-03
0.5	1.75	0.501	10.650	1.34E-02	2.28	3.50E-03	9.93E-03
0.6	2.11	0.603	14.358	1.25E-02	2.75	3.56E-03	8.97E-03
0.7	2.45	0.701	15.632	1.01E-02	3.19	3.65E-03	6.43E-03
0.8	2.80	0.801	16.475	8.13E-03	3.65	3.52E-03	4.47E-03

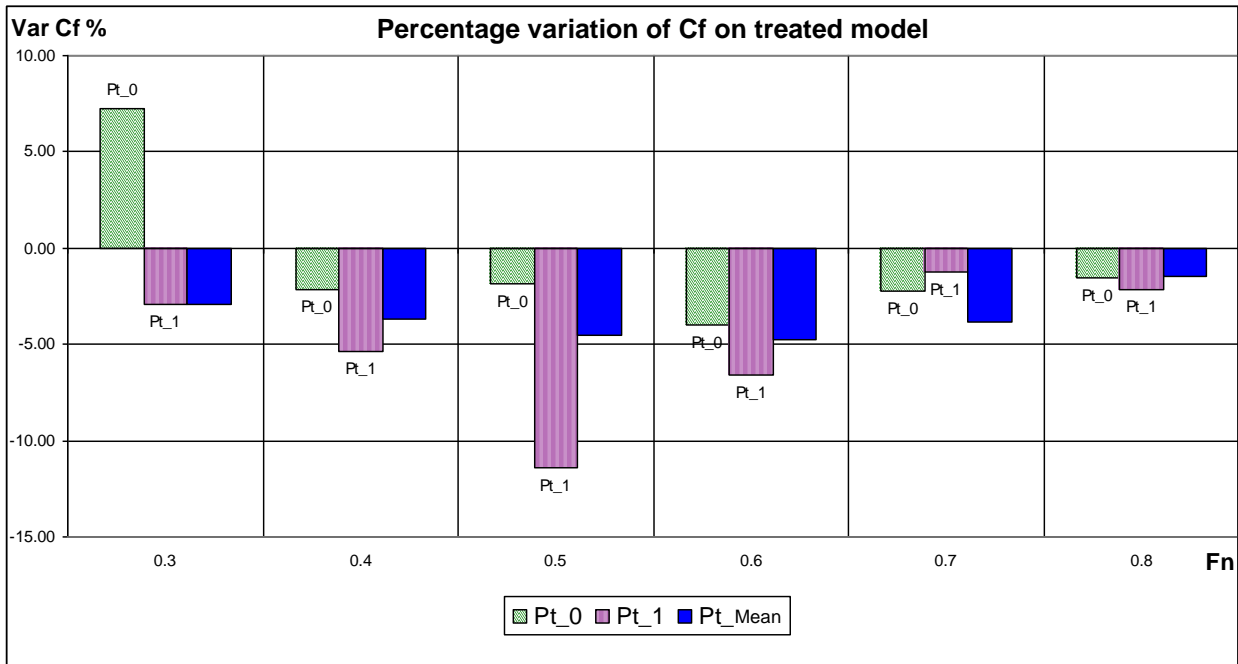
Table 6: Results of the second series of tests, treated model



Graph 1: Total resistance coefficient ( $C_t$ ) as a function of the Froude number



Graph 2: Variation of  $C_f$  as a function of the Froude number



Graph 3: Percentage variation of  $C_f$  on the treated model as a function of the Froude number